O. López, D. Dujic, M. Jones, F. D. Freijedo, J. Doval-Gandoy and E. Levi, "Multidimensional Two-Level Multiphase Space Vector PWM Algorithm and Its Comparison With Multifrequency Space Vector PWM Method," in *IEEE Transactions on Industrial Electronics*, vol. 58, no. 2, pp. 465-475, Feb. 2011, doi: 10.1109/TIE.2010.2047826.

Multidimensional Two-Level Multiphase Space Vector PWM Algorithm and Its Comparison With Multifrequency Space Vector PWM Method

Oscar López, *Member, IEEE*, Drazen Dujic, *Member, IEEE*, Martin Jones, *Member, IEEE*, Francisco D. Freijedo, *Member, IEEE*, Jesús Doval-Gandoy, *Member, IEEE*, and Emil Levi, *Fellow, IEEE*

***Abstract*—A multilevel multiphase space vector pulsewidth modulation (SVPWM) algorithm has been introduced recently, in which the reference is separated into an integer part and a fractional part. The fractional part is, in essence, a two-level multiphase space vector algorithm. This paper shows that, with appropriate adaptations, the fractional part of the general space vector multilevel multiphase PWM can be applied as a stand-alone PWM method in conjunction with two-level voltage-source converters with any number of phases. Simulation results of the five- and six-phase cases are shown, and the new algorithm is compared with another recent multifrequency SVPWM algorithm, which follows the standard approach of selecting the switching vectors and calculating their application times using *dq* planes. The experimental verification is provided using a five-phase two-motor series-connected induction motor drive, supplied from a custom-designed five-phase voltage-source inverter.**

***Index Terms*—Modulation index range, multifrequency pulsewidth modulation (PWM), multiphase voltage-source converter, space vector PWM (SVPWM).**

I. Introduction

MAIN advantages of multiphase machines over their three-phase counterparts are the following: 1) higher efficiency; 2) the greater fault tolerance; and 3) the lower torque pulsation [1]. Multiphase motor drives are of interest for applications where their advantages outweigh the lack of the off-the-shelf availability of both machines and power electronic converters [2]. They have been found to be ideally suited for direct drives in marine propulsion applications [3]–[5] and for drive systems in safety-critical applications, such as the more-electric aircraft [6]–[11]. Other recent applications include electric vehicle propulsion [12]–[15] and locomotive traction [16], [17].

Manuscript received July 16, 2009; revised February 24, 2010; accepted March 24, 2010. Date of publication April 12, 2010; date of current version January 12, 2011. This work was supported in part by the Spanish Ministry of Education and Science under Project DPI2009-07004 and in part by the University of Vigo under Grant "Estadías en centros de investigación."

O. López, F. D. Freijedo, and J. Doval-Gandoy are with the Department of Electronics Technology, University of Vigo, 36310 Vigo, Spain (e-mail: olopez@uvigo.es).

D. Dujic is with the ABB Corporate Research Center, 5405 Baden-Dättwil, Switzerland (e-mail: drazen.dujic@ieee.org).

M. Jones and E. Levi are with the School of Engineering, Technology and Maritime Operations, Liverpool John Moores University, L3 3AF Liverpool, U.K. (e-mail: e.levi@ljmu.ac.uk).

Digital Object Identifier 10.1109/TIE.2010.2047826

Advances in multiphase drives led to the corresponding development of new pulsewidth modulation (PWM) techniques. The carrier-based PWM techniques developed for multiphase systems are rather simple extensions of the techniques developed for three-phase converters [18]–[21]. The extension of the space vector PWM (SVPWM) techniques from three to multiphase systems is however more involved. The classical motor-drive approach selects the switching vectors using reference-related considerations in several 2-D dq planes [22]–[28]. The majority of such techniques is related to two-level converters with a particular number of phases and a single-frequency output. The dq SVPWM for three-level converters is addressed in [27], and the dq SVPWM for a multifrequency output with two-level inverters is addressed in [28]. A recent alternative approach to SVPWM is the selection of the space vectors directly in a multidimensional space [29]. However, the existing approach to the switching vector selection [29], [30] is characterized with the huge computational cost [30]. The algorithm for two-level converters with any number of phases, presented in [31], can deal with multifrequency output and has low computational cost; however, this algorithm requires storing of precalculated tables, and table size increases dramatically with an increase in the number of phases. Recently, three generic multidimensional SVPWM techniques for multilevel multiphase converters with low computational cost, low memory requirements, and capability of multifrequency output generation have been developed [32]–[34]. The modulation techniques in [33] and [34] are specifically for multilevel converters: The former technique takes into account the switching state redundancy present in multilevel topologies, while the latter one reduces distortion in the output waveform due to imbalances in the dc links of multilevel converters. The SVPWM technique in [32], which was the precursor of [33] and [34], makes use of a two-level SVPWM algorithm. This two-level algorithm, which was specifically developed to solve the multilevel problem, is a general two-level multiphase SVPWM technique that can be used as a stand-alone PWM technique with two-level voltage-source converters. Since two-level inverters are, nowadays, customarily used as the supply in multiphase drives, the fractional part of the general multilevel SVPWM algorithm actually has a better prospect for real-world applications than the complete multilevel algorithm.

This paper studies the application of the two-level multiphase SVPWM algorithm developed in [32] to conventional two-level

voltage-source converters. It shows, for the first time, that this algorithm can be used for both sinusoidal and multifrequency output voltage generation with two-level inverters, and provides corresponding experimental proofs. The new multidimensional modulation algorithm has a number of properties inherited from the algorithm in [32]. Thus, it can be used with converters with any number of phases; it has a low computational cost, and it is suitable for online implementation. The range of the modulation index in the linear region of the algorithm is calculated in this paper, and the technique to extend it when the load has the floating neutral point is outlined. The algorithm is simulated with a five- and a six-phase inverter, and it is compared with the recent multifrequency SVPWM algorithm in [28], which carries the switching vector selection in several dq planes. Experimental results, collected from a five-phase two-motor series-connected drive, are given to verify the theoretical analysis.

II. Two-Level Multiphase SVPWM

A. Multidimensional Formulation and Modulation Law

The two-level multiphase SVPWM technique presented in [32] formulates the modulation problem of a P-phase voltage-source converter in a multidimensional space, in which the normalized reference vector

$$\mathbf{v}_r = \left[v_r^1, v_r^2, \ldots, v_r^P\right]^{\mathrm{T}} \tag{1}$$

and the switching state vectors

$$\mathbf{v}_{sj} = \left[v_{sj}^1, v_{sj}^2, \ldots, v_{sj}^P\right]^{\mathrm{T}}, \qquad j = 1, \ldots, P+1 \tag{2}$$

are P-dimensional vectors. The reference vector $\mathbf{v}_r$ gathers the normalized reference voltages of all legs of the converter, which are calculated by dividing the actual reference voltage by the dc-link voltage $v_r^k = \mathbf{V}_r^k / V_{\mathrm{dc}}$. In the same way, the switching vectors $\mathbf{v}_{sj}$ gather the switching states of the legs of the converter. In two-level converters, each leg has only two possible states: zero and one. The lower switch of leg k is on and the upper switch of leg k is off for the case $v_s^k = 0$, whereas in the case $v_s^k = 1$, the switches of the leg k are in the opposite state.

Since the switching states of the power converter stay at discrete states, the SVPWM technique is used to synthesize the reference voltage vector $\mathbf{v}_r$ by means of a sequence of space vectors $\mathbf{v}_{sj}$ during each modulation cycle. Each space vector must be applied during a normalized dwell time t_j in accordance with the following modulation law:

$$\mathbf{v}_r = \sum_{j=1}^{P+1} \mathbf{v}_{sj} t_j, \quad \sum_{j=1}^{P+1} t_j = 1 \tag{3}$$

in which the negative rail of the dc link is the reference voltage point. The actual dwell time T_j corresponding to the switching vector $\mathbf{v}_{sj}$ is obtained from the switching period as $T_j = t_j T$.

If expressions in (3) are rewritten in matrix format, then the following system of linear equations is obtained:

$$\begin{bmatrix} 1 \\ v_r^1 \\ v_r^2 \\ \vdots \\ v_r^P \end{bmatrix} = \underbrace{\begin{bmatrix} 1 & 1 & \cdots & 1 \\ v_{s1}^1 & v_{s2}^1 & \cdots & v_{sP+1}^1 \\ v_{s1}^2 & v_{s2}^2 & \cdots & v_{sP+1}^2 \\ \vdots & \vdots & \ddots & \vdots \\ v_{s1}^P & v_{s2}^P & \cdots & v_{sP+1}^P \end{bmatrix}}_{\mathbf{D}} \begin{bmatrix} t_1 \\ t_2 \\ \vdots \\ t_{P+1} \end{bmatrix}. \tag{4}$$

The two-level multiphase algorithm in [32] finds the coefficient matrix $\mathbf{D}$ that allows solving the aforementioned system of linear equations, and then, it calculates the solution dwell times. The coefficients of matrix $\mathbf{D}$ only take the values zero or one because the converter only has two levels.

The application of the multidimensional two-level multiphase SVPWM algorithm requires calculation of a permutation matrix $\mathbf{P}$ that sorts the elements of the reference vector $\mathbf{v}_r$ in descending order

$$\mathbf{P} \begin{bmatrix} 1 \\ \mathbf{v}_r \end{bmatrix} = \begin{bmatrix} 1 \\ \hat{\mathbf{v}}_r \end{bmatrix} \tag{5}$$

where $\hat{\mathbf{v}}_r = [\hat{v}_r^1, \hat{v}_r^2, \ldots, \hat{v}_r^P]^{\mathrm{T}}$ is the reference vector after sorting is completed, in which

$$\hat{v}_r^1 \geq \cdots \geq \hat{v}_r^{k-1} \geq \hat{v}_r^k \geq \cdots \geq \hat{v}_r^P. \tag{6}$$

In [32], the reference vector for the two-level multiphase SVPWM is the fractional part of the reference vector, and consequently, all the components of that vector are always in the interval [0, 1). When the two-level SVPWM algorithm is applied as a stand-alone algorithm, then its reference voltage can be of any value, and the constraints $\hat{v}_r^1 \geq 0$ and $\hat{v}_r^P < 1$ in [32] no longer apply. The permutation matrix and the sorted vector $\hat{\mathbf{v}}_r$ can be readily obtained at the same time by making row-switching transformations in the following augmented matrix:

$$\left[\begin{array}{c|c} 1 & \\ \mathbf{v}_r & \mathbf{I} \end{array}\right] \xrightarrow[\text{transformations}]{\text{Row}-\text{switching}} \left[\begin{array}{c|c} 1 & \\ \hat{\mathbf{v}}_r & \mathbf{P} \end{array}\right] \tag{7}$$

where $\mathbf{I}$ is the $(P+1) \times (P+1)$ identity matrix. The goal in the row-switching transformation is to exchange the columns of the augmented matrix in order to sort the components of the vector $\mathbf{v}_r$ in the first column. It is important to remark that the first row is never moved. The resulting augmented matrix includes both the sorted vector $\hat{\mathbf{v}}_r$ and the permutation matrix $\mathbf{P}$.

The coefficient matrix $\mathbf{D}$ is calculated with the permutation matrix $\mathbf{P}$ as

$$\mathbf{D} = \mathbf{P}^{\mathrm{T}} \hat{\mathbf{D}} \tag{8}$$

where $\hat{\mathbf{D}}$ is the following upper triangular matrix:

$$\hat{\mathbf{D}} = \begin{bmatrix} 1 & 1 & \cdots & 1 \\ & 1 & \cdots & 1 \\ & & \ddots & \vdots \\ 0 & & & 1 \end{bmatrix}. \tag{9}$$

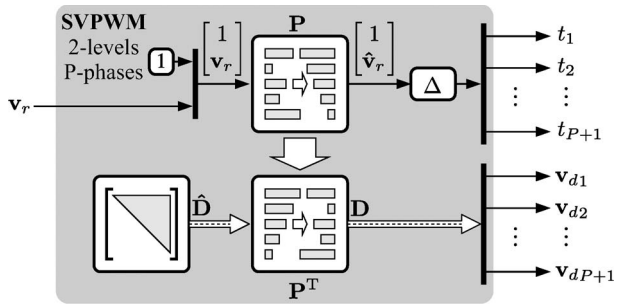

Fig. 1. Block diagram of the two-level multiphase SVPWM.

Since the matrix $\mathbf{P}^{\mathrm{T}}$ applies to the matrix $\mathbf{D}$, the inverse set of row-switching transformation done in (7), the matrix multiplication in (8) can be avoided if the operations carried out to sort the reference vector $\mathbf{v}_r$ are stored and then applied in inverse order to the matrix $\mathbf{D}$ [32]. Finally, the dwell times are calculated from $\hat{\mathbf{v}}_r$ as

$$t_j = \begin{cases} 1 - \hat{v}_r^1, & \text{if } j = 1 \\ \hat{v}_r^{j-1} - \hat{v}_r^j, & \text{if } 2 \leq j \leq P \\ \hat{v}_r^P, & \text{if } j = P+1. \end{cases} \tag{10}$$

Since constraints $\hat{v}_r^1 \geq 0$ and $\hat{v}_r^P < 1$ no longer apply, then some reference vectors can lead to a negative dwell time. In this case, the reference vector is in the overmodulation region, and it cannot be accurately synthesized, which requires an investigation of the modulation index range of the stand-alone SVPWM algorithm.

In summary, as it is shown in Fig. 1, the steps of the multidimensional two-level multiphase SVPWM algorithm are the following:

1) calculation of the normalized reference vector $\mathbf{v}_r$;
2) calculation of the sorted reference vector $\hat{\mathbf{v}}_r$ and the permutation matrix $\mathbf{P}$ by means of (7);
3) rearrangement of the rows of the triangular matrix $\hat{\mathbf{D}}$ to obtain the matrix $\mathbf{D}$ by means of (8);
4) extraction of the switching vectors $\mathbf{v}_{dj}$ from the matrix $\mathbf{D}$ by taking into account the expression in (4);
5) calculation of the time corresponding to each switching vector from the components of the vector $\hat{\mathbf{v}}_r$ by means of (10).

The application of the algorithm is illustrated by considering an arbitrary reference voltage for each leg of a five-phase inverter: $0.69V_{\mathrm{dc}}$ for leg a, $0.60V_{\mathrm{dc}}$ for leg b, $0.11V_{\mathrm{dc}}$ for leg c, $0.21V_{\mathrm{dc}}$ for leg d, and $0.34V_{\mathrm{dc}}$ for leg e. The values are given with respect to the negative rail of the dc link. In this case, the normalized reference vector for the algorithm is

$$\mathbf{v}_r = [0.69, 0.60, 0.11, 0.21, 0.34]^{\mathrm{T}}. \tag{11}$$

After carrying out the row-switching transformations on the augmented matrix made with $\mathbf{v}_r$ and the identity 6×6 matrix, as it was depicted in (7), the following sorted vector:

$$\hat{\mathbf{v}}_r = [0.69, 0.60, 0.34, 0.21, 0.11]^{\mathrm{T}} \tag{12}$$

and the following permutation matrix:

$$\mathbf{P} = \begin{bmatrix} 1 & 0 & 0 & 0 & 0 & 0 \\ 0 & 1 & 0 & 0 & 0 & 0 \\ 0 & 0 & 1 & 0 & 0 & 0 \\ 0 & 0 & 0 & 0 & 0 & 1 \\ 0 & 0 & 0 & 0 & 1 & 0 \\ 0 & 0 & 0 & 1 & 0 & 0 \end{bmatrix} \tag{13}$$

are obtained. From (8), the matrix $\mathbf{D}$ is calculated as

$$\mathbf{D} = \mathbf{P}^{\mathrm{T}}\hat{\mathbf{D}} = \begin{bmatrix} 1 & 1 & 1 & 1 & 1 & 1 \\ 0 & 1 & 1 & 1 & 1 & 1 \\ 0 & 0 & 1 & 1 & 1 & 1 \\ 0 & 0 & 0 & 0 & 0 & 1 \\ 0 & 0 & 0 & 0 & 1 & 1 \\ 0 & 0 & 0 & 1 & 1 & 1 \end{bmatrix} \tag{14}$$

and the switching vector sequence is extracted from this matrix, taking into account its definition given in (4)

$$\begin{aligned} \mathbf{v}_{d1} &= [0,0,0,0,0]^{\mathrm{T}} \\ \mathbf{v}_{d2} &= [1,0,0,0,0]^{\mathrm{T}} \\ \mathbf{v}_{d3} &= [1,1,0,0,0]^{\mathrm{T}} \\ \mathbf{v}_{d4} &= [1,1,0,0,1]^{\mathrm{T}} \\ \mathbf{v}_{d5} &= [1,1,0,1,1]^{\mathrm{T}} \\ \mathbf{v}_{d6} &= [1,1,1,1,1]^{\mathrm{T}}. \end{aligned} \tag{15}$$

As expected, consecutive vectors of the sequence are adjacent. Therefore, the number of switchings is minimized. Finally, the switching times are calculated from the ordered reference vector $\hat{\mathbf{v}}_r$ by means of the expression in (10)

$$\begin{aligned} t_1 &= 1 - \hat{v}_r^a = 0.31 \\ t_2 &= \hat{v}_r^a - \hat{v}_r^b = 0.09 \\ t_3 &= \hat{v}_r^b - \hat{v}_r^c = 0.26 \\ t_4 &= \hat{v}_r^c - \hat{v}_r^d = 0.13 \\ t_5 &= \hat{v}_r^d - \hat{v}_r^e = 0.10 \\ t_6 &= \hat{v}_r^e = 0.11. \end{aligned} \tag{16}$$

B. Modulation Index Range

The reference vector cannot be accurately synthesized, i.e., it lies in the overmodulation region, if some of the switching vectors have a negative dwell time. Dwell times from t_2 to t_P are always positive because they are calculated from the components of $\hat{\mathbf{v}}_r$ by means of (10), and the components of $\hat{\mathbf{v}}_r$ fulfill the expression in (6). The only dwell times that can be negative are t_1 and t_{P+1}. Therefore, the following rule applies in order to determine if the reference vector lies in the overmodulation region:

$$t_1 < 0 \quad t_{P+1} < 0. \tag{17}$$

From (6), the first and the last components of the sorted reference vector can be written as

$$\hat{v}_r^1 = \max_{k=1,\ldots,P} \left(v_r^k\right) \tag{18}$$

$$\hat{v}_r^P = \min_{k=1,\ldots,P} \left(v_r^k\right). \tag{19}$$

Thus, $t_1 = 1 - \max_k(v_r^k)$, and $t_{P+1} = \min_k(v_r^k)$. Consequently, the rule in (17) can be rewritten as a function of the reference voltages as

$$\min_{k=1,\ldots,P} \left(v_r^k\right) < 0 \quad \max_{k=1,\ldots,P} \left(v_r^k\right) > 1. \tag{20}$$

Hence, the reference vector $\mathbf{v}_r$ lies in the overmodulation region of the modulation index if some of its components are outside the interval [0, 1]. If the modulation index is defined as the ratio of the peak-to-peak fundamental of the output voltage to the dc-link voltage $m = V_{\rm pp}/V_{\rm dc}$, then the modulation index of the multidimensional two-level multiphase SVPWM algorithm is limited to

$$m \leq 1. \tag{21}$$

In the case of multifrequency output, a modulation index is defined for each frequency component, i.e., $m_i = V_{{\rm pp}_i}/V_{\rm dc}$. In this case, the modulation indexes are limited by the expression

$$\sum_{i=1}^{Q} m_i \leq 1 \tag{22}$$

where $Q = (P-1)/2$ if the number of phases is odd and $Q = P/2 - 1$ if P is an even number. This is the same limit as with the classical sinusoidal carrier-based PWM technique. The mathematical demonstration of (21) and (22) is provided in the Appendix.

C. Modulation Index Extension

The switching vector sequence obtained with the modulation law in (3) guarantees that the reference leg voltage and the cycle-by-cycle averaged output leg voltage are equal in the linear region of the modulation index. Consequently, the reference vector and the averaged output vector obtained with the SVPWM algorithm have the same homopolar and nonhomopolar components. Therefore, this algorithm can be used both with converters with neutral and without load neutral wire. Nevertheless, in the latter case, if the voltage of the neutral point of the load is not a constraint, then the homopolar component of the output voltage can be modified to increase the modulation index range.

If the homopolar component h is added to the output voltage by applying the modified reference vector $\mathbf{v}_r' = [v_r^1 + h, v_r^2 + h, \ldots, v_r^P + h]^{\rm T}$ to the SVPWM algorithm, then the switching vector sequence does not change. It is because the row-switching transformations to sort $\mathbf{v}_r$ and $\mathbf{v}_r'$ are the same, and consequently, matrices $\mathbf{P}$ and $\mathbf{D}$ are the same as well.

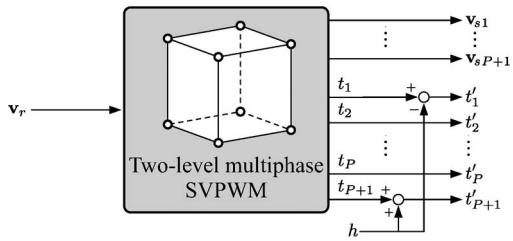

Fig. 2. Modification of the homopolar component of the output voltage.

From (10), the dwell times corresponding to the new reference vector are

$$t_j' = \begin{cases} t_1 - h, & \text{if } j = 1 \\ t_j, & \text{if } 2 \leq j \leq P \\ t_{P+1} + h, & \text{if } j = P+1. \end{cases} \tag{23}$$

Therefore, as Fig. 2 shows, the homopolar component of the output voltage can be modified by changing the dwell times corresponding to the first and the last elements of the switching vector sequence. Since those are the only dwell times that are taken into account in the overmodulation rule in (17), it is possible to correct a negative value in t_1' or t_{P+1}' to avoid an eventual overmodulation situation of the SVPWM algorithm. This correction is carried by selecting a value of h in the range

$$-t_{P+1} \leq h \leq t_1. \tag{24}$$

Such a correction is not possible if the length of this interval is negative because, in this case, there does not exist any value of h that provides positive values for t_1' and t_{P+1}' at the same time. Consequently, the condition

$$t_1 + t_{P+1} < 0 \tag{25}$$

can be used to check if the reference vector lies in the overmodulation region when the correction of the dwell times is carried out. This rule is less restrictive than the rule in (17). If expressions in (18) are taken into account, then the aforementioned overmodulation condition can be rewritten in terms of the normalized reference vector as

$$\max_{k=1,\ldots,P} \left(v_r^k\right) - \min_{k=1,\ldots,P} \left(v_r^k\right) > 1. \tag{26}$$

If symmetrical multiphase systems where the phase shift between consecutive phases is $2\pi/P$ and single-frequency output are considered, then the modulation index is limited to

$$m \leq \begin{cases} 1/\cos\left(\frac{\pi}{2P}\right), & \text{if } P \text{ is odd} \\ 1, & \text{if } P \text{ is even} \end{cases} \tag{27}$$

which is the limit of the sinusoidal carrier-based PWM with harmonic injection technique [18]. In the case of multifrequency output, the modulation indexes of all components are limited by the expressions

$$\sum_{i=1}^{Q} m_i \left|\sin(ni\pi/P)\right| \leq 1, \qquad \text{for } n = 1, \ldots, N \tag{28}$$

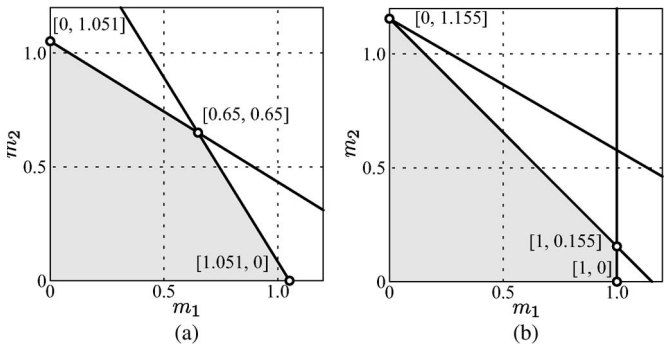

Fig. 3. Area of the permissible modulation index pairs. (a) Five-phase system. (b) Six-phase system.

where $N = (P-1)/2$ if P is odd and $N = P/2$ if P is even. The mathematical demonstration of (27) and (28) is provided in the Appendix.

It is interesting at this point to address the result of (28) in more detail. Consider, for example, a five-phase system. According to (28)

$$\begin{cases} m_1 \sin(\pi/5) + m_2 \sin(2\pi/5) \le 1 \\ m_1 \sin(2\pi/5) + m_2 \sin(4\pi/5) \le 1. \end{cases} \tag{29}$$

Equation (29) defines the area shown in Fig. 3(a) of the permissible modulation index pairs in the $m_1 m_2$ plane, which satisfy simultaneously both those in (29). In the limit $m_1 = m_2 = m_{\max}$ and solution of (29) is $m_{\max} = 0.6498$. This means that the sum of the two modulation indexes in the limit of the linear modulation region is equal to 1.2996, which is considerably more than for the single-frequency operation ($m_{\max} = 1.0515$). This result shows that the multidimensional two-level SVPWM algorithm enables full utilization of the dc bus voltage. It is also in full agreement with the general study of the limits of the dc bus voltage utilization in the linear modulation region, reported in [35], for multiphase inverter-fed systems. The analysis in [35] is the only known study. It has been based on a simple physical reasoning and was independent of the PWM method. On the other hand, the analysis here for a specific multidimensional SVPWM yields the same results so that (28), in essence, verifies the findings in [35] and vice versa.

In the case of a six-phase system and according to (28), the area of the permissible modulation index pairs is defined by

$$\begin{cases} m_1 \sin(\pi/6) + m_2 \sin(2\pi/6) \le 1 \\ m_1 \sin(2\pi/6) + m_2 \sin(4\pi/6) \le 1 \\ m_1 \sin(3\pi/6) + m_2 \sin(6\pi/6) \le 1. \end{cases} \tag{30}$$

This area is shown in Fig. 3(b). As can be seen, the sum of the two modulation indexes is restricted to no more than 1.1547. The individual maximum values are $m_{1\max} = 1$ and $m_{2\max} = 1.1547$. This means that, although the sum of the two modulation indexes in the limit of the linear modulation region is equal to 1.1547, the operation with $m_2 = 0$ leads to the maximum value of m_1 of only $m_{1\max} = 1$ (which is the limit for the single-frequency operation). On the other hand, the operation with $m_{2\max} = 1.1547$ (the same limit as for the three-phase case) is possible when $m_1 = 0$.

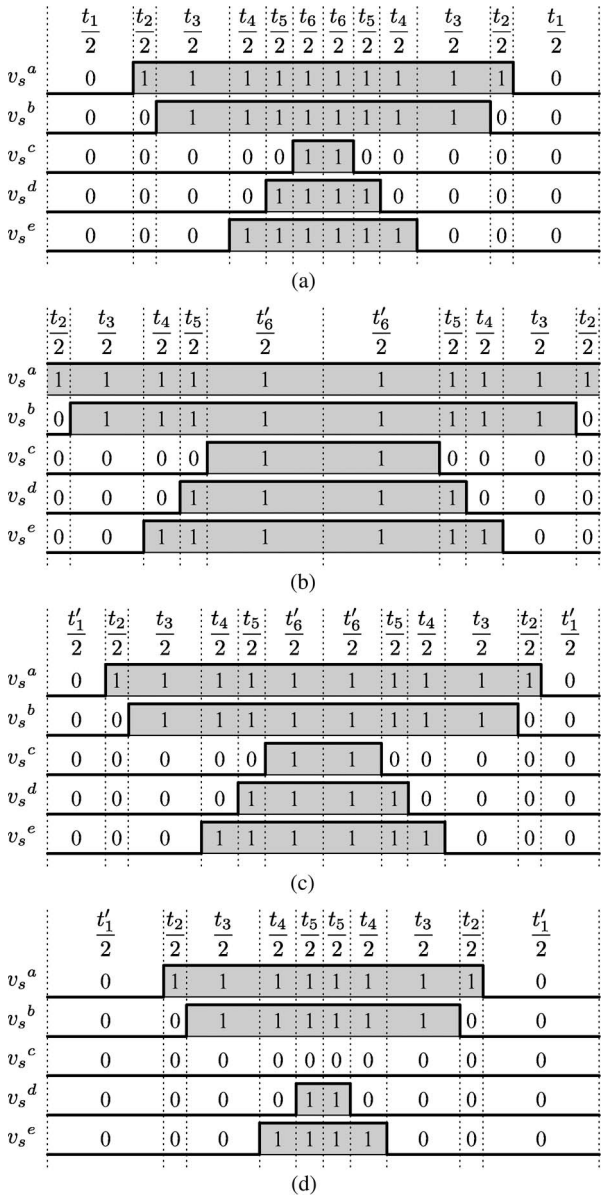

Fig. 4. Switching patterns. (a) Case 1: No dwell time correction. (b) Case 2a: The first switching vector is not used. (c) Case 2b: Balanced dwell times of the first and the last switching vectors. (d) Case 2c: The last switching vector is not used.

D. Algorithm Simulation

The multidimensional two-level SVPWM algorithm was simulated for single-frequency output with a five-phase inverter for four cases.

1) Algorithm without dwell time correction ($h = 0$).
2) Algorithm with the following dwell time corrections:
   a) Correction with $h = t_1$; therefore, $t'_1 = 0$, and $t'_{P+1} = t_1 + t_{P+1}$.
   b) Correction with $h = (1/2)(t_1 + t_{P+1})$; hence, $t'_1 = t'_{P+1} = (1/2)(t_1 + t_{P+1})$.
   c) Correction with $h = -t_{P+1}$; therefore, $t'_1 = t_1 + t_{P+1}$, and $t'_{P+1} = 0$.

Fig. 4 shows the switching patterns obtained, in the four cases, with the same normalized reference vector considered in the previous example $\mathbf{v}_r = [0.69, 0.60, 0.11, 0.21, 0.34]^{\mathrm{T}}$.

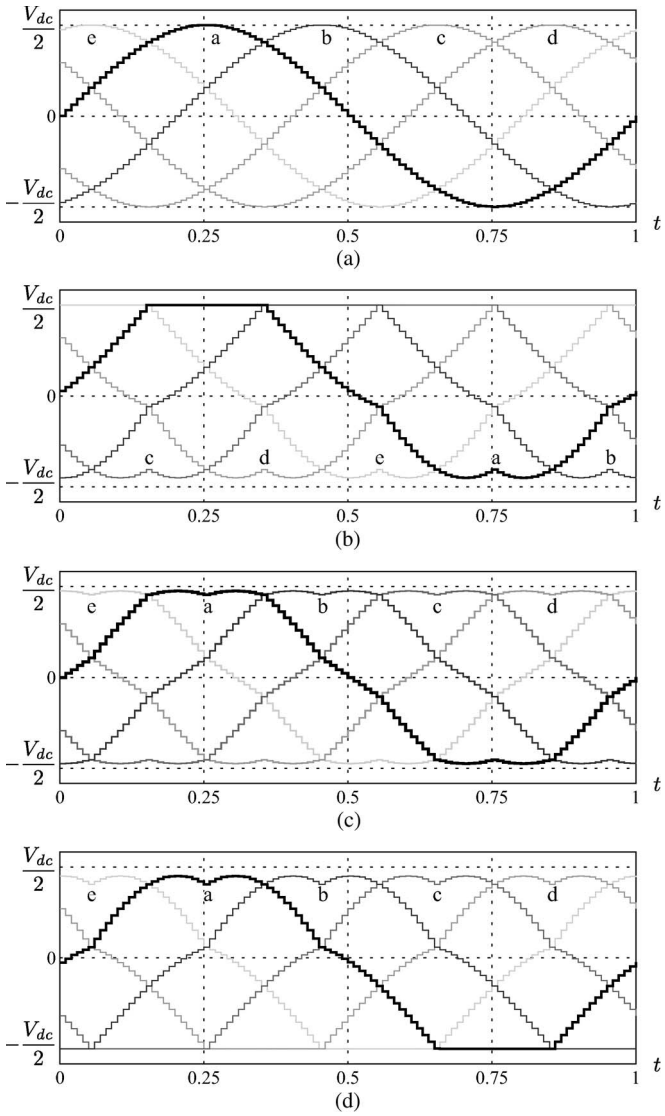

Fig. 5. Cycle-by-cycle averaged output leg voltage. (a) Case 1: No dwell time correction. (b) Case 2a: The first switching vector is not used. (c) Case 2b: Balanced dwell times of the first and the last switching vectors. (d) Case 2c: The last switching vector is not used.

The switching vectors have been arranged symmetrically in the switching period. Fig. 4(a) shows the switching pattern obtained in case 1 with the switching vectors in (15) and the switching times in (16), where $t_1 = 0.31$ and $t_6 = 0.11$. In case 2a, the dwell time of the first switching vector is always zero, so such a vector is never used, as it is shown in Fig. 4(b), where $t'_1 = 0$ and $t'_6 = 0.42$. Fig. 4(c) shows case 2b, where the dwell times of the first and the last vector are balanced $t'_1 = t'_6 = 0.21$. In case 2c, the last vector is not used because it has a zero dwell time, as it is shown in Fig. 4(d), where $t'_1 = 0.42$ and $t'_6 = 0$. In cases 2a and 2c, there is always one leg that keeps constant its switching state throughout the switching period, and as a result, the switching losses in those cases are reduced.

Fig. 5 shows the cycle-by-cycle averaged output waveforms in the four cases explained previously when the reference is a purely sinusoidal wave with unit peak-to-peak amplitude $(m = 1)$. In the simulations, the output leg voltages of the converters are measured with respect to the midpoint of the dc link, and a switching frequency that is 20 times the output fundamental has been considered. Fig. 5(a) shows case 1 in which there is no correction of the dwell times; thus, the averaged output voltage is equal to the reference voltage. In this case, the filtered output leg voltage is the same as that with the carrier-based PWM technique [18]. Fig. 5(b)–(d) shows the cases that include dwell time correction. In all of them, the modulation index can be increased by up to 5.1% within the linear region. The corrections performed in cases 2a and 2c provide a discontinuous PWM, whereas a continuous PWM is obtained in cases 1 and 2b. The filtered output leg voltage in case 2b is the same as that with the carrier-based PWM technique with triangular zero-sequence injection [20].

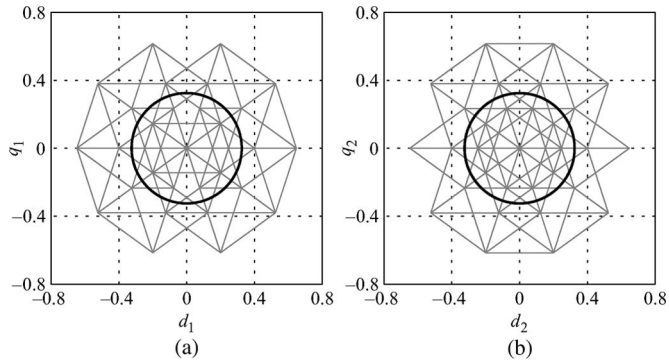

Fig. 6. Trajectories of the output voltage of the five-phase converter in the dq planes. (a) d_1q_1 plane. (b) d_2q_2 plane.

The algorithm was simulated in the case of multifrequency output for five- and six-phase converters. In the following simulations, the dwell time correction of case 2b, shown in Fig. 5(c), was used to extend the modulation index range. Fig. 6 shows the trajectories of the output voltage vectors in the two dq planes corresponding to a five-phase system. The thin traces in gray correspond to the unfiltered output voltage, and the thick traces in black are the trajectories of the cycle-by-cycle averaged output voltage. In the d_1q_1 plane, a reference with the modulation index $m_1 = 0.64984$ and a fundamental frequency of 50 Hz was considered. In the d_2q_2 plane, a reference with the same modulation index $m_2 = 0.64984$ and a fundamental frequency of 150 Hz was considered. This pair of modulation indexes corresponds to the limit case obtained in Section II-C. Therefore, as expected, the trajectory of the filtered voltage is a circle in each plane because the multiphase SVPWM operates always in the linear region (essentially, in the limit).

Fig. 7 shows the trajectories of the output voltage vectors in the two dq planes corresponding to a six-phase system. In the d_1q_1 plane, a modulation index $m_1 = 1$ and a fundamental frequency of 50 Hz were considered. In the d_2q_2 plane, the modulation index $m_2 = 0.1547$ and a fundamental frequency of 150 Hz were considered. This pair of modulation indexes corresponds to the limit case obtained in Section II-C for six-phase systems. Therefore, as expected, the trajectory of the filtered voltage is a circle in each plane. The trajectory of the averaged output voltage in the 0-axis, not shown in the figures, is equal to zero. Consequently, the multidimensional SVPWM operates properly.

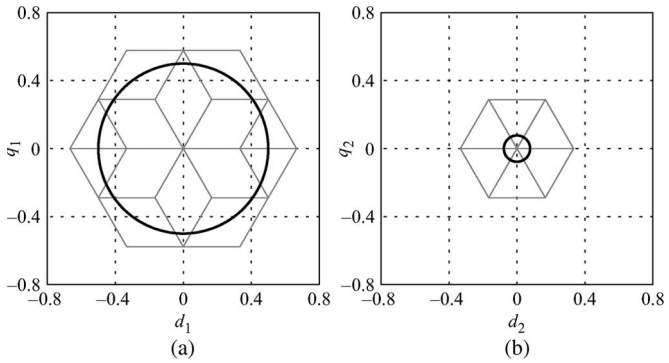

Fig. 7. Trajectories of the output voltage of the six-phase converter in the dq planes. (a) d_1q_1 plane. (b) d_2q_2 plane.

III. Comparison With Multifrequency SVPWM Algorithm

The customary approach in variable-speed motor drives consists in decomposing the multidimensional space in several dq planes, using either real decoupling transformations or a symmetrical component approach [36], [37]. A very demanding situation for such PWM techniques arises in multimotor series-connected multiphase drive systems with a single voltage-source inverter [38]. In this case, each dq plane is used to control one machine of the system, and selecting an appropriate switching vector sequence is complex because magnitudes and frequencies of the reference voltages in all dq planes are completely independent one from the other. The multifrequency SVPWM algorithm presented in [28] allows selecting the switching vectors and calculating their dwell times in two-motor series-connected five-phase drives. This algorithm takes the magnitude and the angle of the reference voltage in each dq plane and selects in each plane four active vectors, as proposed in [39]. It requires dividing each dq plane in ten sectors and taking the two mediums and the two large vectors corresponding to the sector in which the reference vector lies. The four active vectors of the first dq plane (first machine) plus the four active vectors of the second dq plane (second machine) are reduced to only four active vectors by summing the duty cycles of both planes on a per-leg basis [28]. It results in a switching vector sequence with six adjacent vectors arranged symmetrically in the switching period. The switching vector sequence includes two zero vectors and four active vectors, where the first and the last ones are always the zero vectors $[0,0,0,0,0]^{\mathrm{T}}$ and $[1,1,1,1,1]^{\mathrm{T}}$, respectively. The same dwell time is used for both of them.

The two-level SVPWM algorithm, elaborated in this paper, can be used with converters with any number of phases. It provides a space vector sequence made with $P+1$ adjacent vectors because the sequence is obtained by reordering the columns of the triangular matrix $\hat{\mathbf{D}}$. The difference between two adjacent vectors is only one bit; consequently, the algorithm minimizes the number of switchings. In addition, it has a low computational cost, which grows slightly with the phase number because of the greater number of elements in $\mathbf{v}_r$ that must be sorted out. Therefore, it is well suited for real-time implementation in low-cost devices.

With the multidimensional SVPWM algorithm presented in this paper, the reference voltage for each leg can be an arbitrary waveform. Consequently, it is possible to synthesize an output voltage that contains a certain number of sinusoidal components like with the multifrequency SVPWM algorithm. The numbers of switching vectors used by the multifrequency and the multidimensional SVPWM algorithms are the same. In addition, in the multidimensional SVPWM algorithm, the first and the last vectors of the switching sequence are always the zero vectors $\mathbf{v}_{s1} = [0,0,\ldots,0]^{\mathrm{T}}$ and $\mathbf{v}_{sP+1} = [1,1,\ldots,1]^{\mathrm{T}}$, respectively. This is so because the switching vector sequence is obtained from matrix $\mathbf{D}$ after reordering all rows of the triangular matrix $\hat{\mathbf{D}}$ except the first one. The remaining vectors $\mathbf{v}_{s2}$ to $\mathbf{v}_{sP}$ are all active vectors. Therefore, for a five-phase converter, if the switching pattern is obtained as in case 2b of the previous section, then both algorithms have the following similarities.

1) Both use four active vectors.
2) The first and the last switching vectors of the sequence in both algorithms are always $[0,0,0,0,0]^{\mathrm{T}}$ and $[1,1,1,1,1]^{\mathrm{T}}$, respectively.
3) Both balance the dwell time of the zero vectors.
4) Both arrange the switching vectors symmetrically within the switching period.

The differences between the two modulation techniques are the following.

1) They use a different frame for the reference voltage. The multidimensional algorithm requires the values of the reference voltage for each leg, while the multifrequency one requires the amplitude and phase of the vectors in every dq plane.
2) The multidimensional SVPWM algorithm has a lower computational cost. However, if the reference voltage is given in the dq frame, then the required change of the reference frame means that both algorithms will ultimately have a similar computational cost.
3) The result of the multidimensional SVPWM is a sequence of switching vectors with their corresponding dwell times, whereas the multifrequency SVPWM algorithm provides the duty cycles of the transistors of the inverter legs. Therefore, the latter algorithm is better suited for implementation in a digital signal processor (DSP) that includes built-in PWM units, and the former one is suitable for a field-programmable gate array, where the PWM units are not included.
4) The multidimensional algorithm allows eliminating the low-order voltage harmonics in the load neutral point voltage if the dwell times of the switching vectors are not corrected.

The reference vector $\mathbf{v}_r = [0.69, 0.60, 0.11, 0.21, 0.11]^{\mathrm{T}}$ of the example in the previous section corresponds to a reference vector with an amplitude of $|V_1| = 0.3V_{\mathrm{dc}}$ and an angle of $\phi_1 = 15^\circ$ in the first dq plane, and a reference vector with an amplitude of $|V_2| = 0.8V_{\mathrm{dc}}$ and an angle of $\phi_2 = 85^\circ$ in the second dq plane. In this case, the duty cycles obtained with the multifrequency SVPWM algorithm for the legs of the converter are $d^a = 0.79$, $d^b = 0.71$, $d^c = 0.21$,

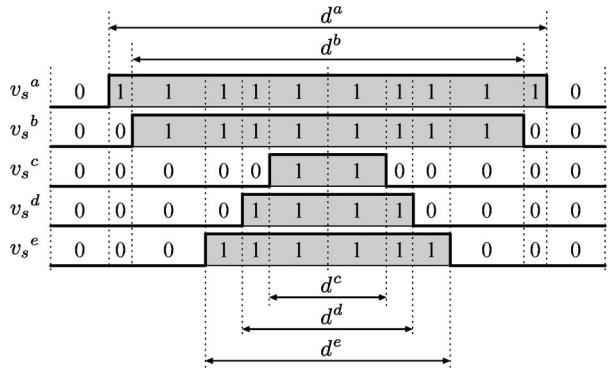

Fig. 8. Switching pattern with the multifrequency SVPWM algorithm.

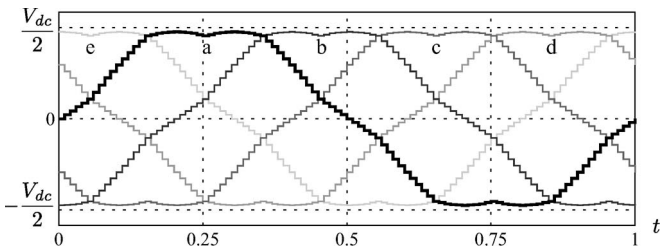

Fig. 9. Cycle-by-cycle averaged output leg voltage with the multifrequency SVPWM algorithm.

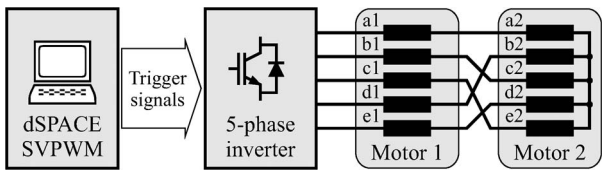

Fig. 10. Experimental setup.

$d^d = 0.31$, and $d^e = 0.44$ which correspond to the switching vector sequence $[0,0,0,0,0]^{\mathrm{T}}$, $[1,0,0,0,0]^{\mathrm{T}}$, $[1,1,0,0,0]^{\mathrm{T}}$, $[1,1,0,0,1]^{\mathrm{T}}$, $[1,1,0,1,1]^{\mathrm{T}}$, and $[1,1,1,1,1]^{\mathrm{T}}$. Fig. 8 shows the switching pattern obtained in this case that is identical to the pattern obtained in Fig. 4(c) corresponding to case 2b of the multidimensional SVPWM algorithm. Fig. 9 shows the cycle-by-cycle averaged output leg voltage with a modulation index equal to one in the first dq plane and a zero reference for the second dq plane. The results obtained are again identical to the results in Fig. 5(c) corresponding to case 2b of the previous section. Both algorithms have been simulated in many different cases providing always the same results, regardless of the fact that they follow very different approaches.

IV. Experimental Results

For the purpose of experimental verification of the multidimensional SVPWM, the testing was done with a two-motor five-phase series-connected induction motor drive. The experimental setup is shown in Fig. 10. It includes a dSPACE platform where the algorithm has been implemented, a five-phase inverter, and two induction motors. The ten PWM trigger signals, with a frequency of 10 kHz, have been generated with the DS5101 Digital Waveform Output board. A more detailed explanation of the inverter, the load, and the operating principles of this multimotor drive can be found in [40]–[42].

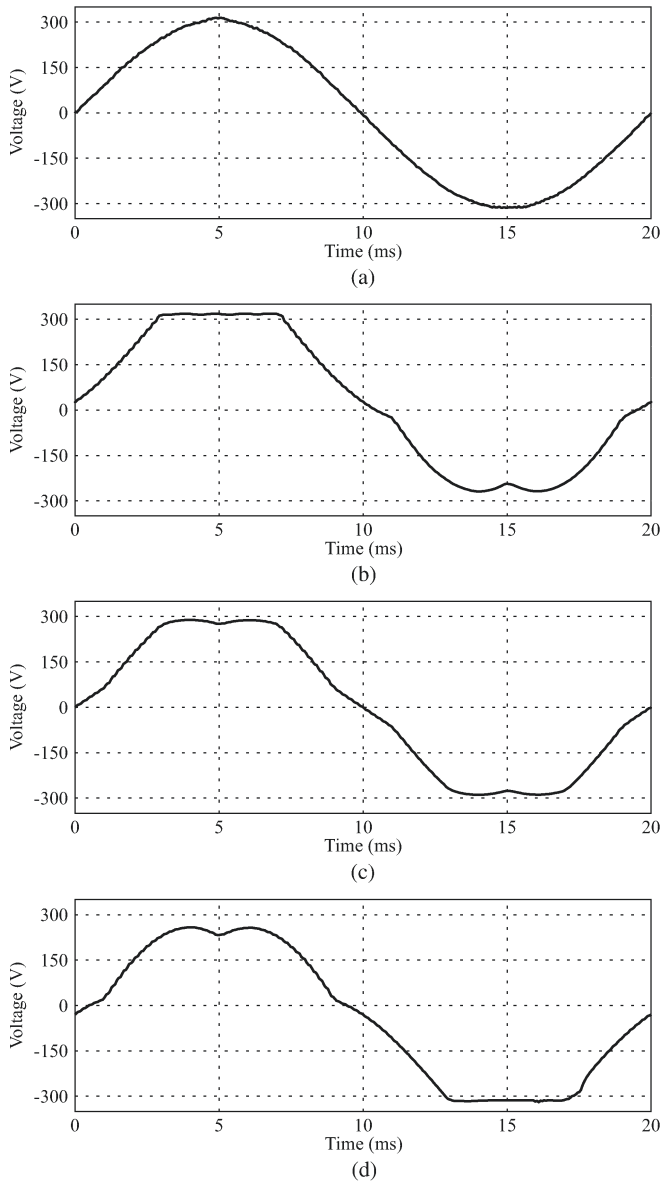

Fig. 11. Filtered leg a voltage with a purely sinusoidal reference. (a) Case 1: No dwell time correction. (b) Case 2a: First switching vector not used. (c) Case 2b: Balanced dwell times. (d) Case 2c: Last switching vector not used.

The drive system is operated in open-loop speed control mode, and the V/Hz ratio is held constant. The inverter dead time is not compensated in the inverter control, and this can cause some undesirable effects, particularly at low reference voltage values [43], [44]. More detailed considerations are however beyond the scope of this paper. It suffices to say that the impact of dead time on the results presented here is very small since all the studied cases involve operation at high modulation index values.

Fig. 11 shows the filtered voltage of leg a measured with respect to the midpoint of the dc link when the reference is a sinusoidal wave with $m = 1$. Voltages have been filtered with a low-pass filter of 1.6-kHz cutoff frequency. The experimental measurements agree with the simulation results shown in Fig. 5(a) and (c) for the cases without and with zero-sequence injection.

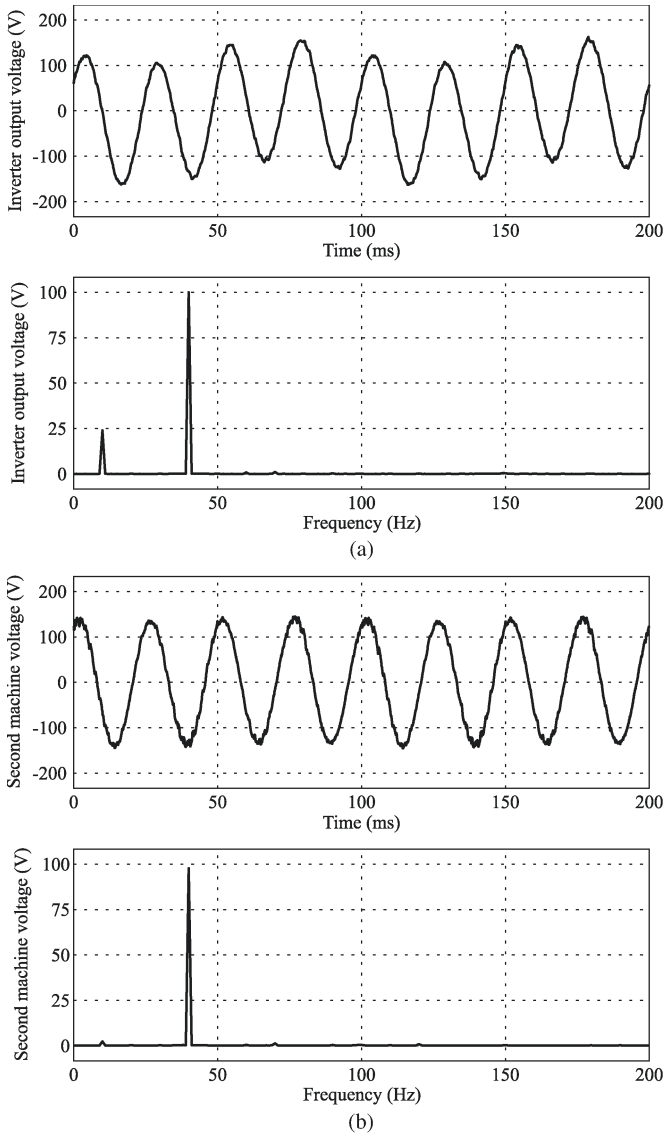

Fig. 12. Measured waveforms and spectra of the phase voltages. (a) Inverter output voltage. (b) Second machine voltage.

Fig. 12 shows the multifrequency output case with the references $f_1 = 10$ Hz and $V_1 = 25$ V for the first machine and $f_2 = 40$ Hz and $V_2 = 100$ V for the second machine. The inverter output voltage spectrum shows two components of frequencies 10 and 40 Hz with the corresponding amplitudes of 25 and 100 V, respectively. The operating point and the experimental results of the multidimensional SVPWM algorithm are equal to the operating point and the experimental results obtained in the third case considered in [28] for the validation of the multifrequency SVPWM algorithm.

V. Conclusion

In this paper, the two-level multiphase SVPWM algorithm developed for a recent multilevel multiphase SVPWM algorithm has been adapted and applied to two-level voltage-source converters. This is a multidimensional algorithm with a low computational cost that can be used with converters with any number of phases. The direct application of the algorithm provides a modulation range in the linear region from zero to one. The linear region can be extended by correcting the dwell times of the switching vectors if the converter has an odd number of phases and the neutral point of the load is floating. The algorithm was simulated and verified by means of a five-phase voltage-source inverter. The new algorithm was also compared with a previous multifrequency SVPWM algorithm that carries the vector selection in individual dq planes. It was shown that both approaches provide the same results.

Appendix
Proof of Modulation Index Range Equations

The control of a multiphase system can be carried out in a set of Q dq planes [1], where $Q = (P-1)/2$, if the number of phases is an odd number, and $Q = P/2 - 1$, if P is an even number. In steady state, the inverter output voltage is composed of a set of sinusoidal waves, with each one mapping to a different dq plane. If a system with a spatial displacement between any consecutive two phases $\alpha = 2\pi/P$ is considered, then the reference voltage for each phase $k = 1, \ldots, P$ can be written as

$$v_r^k = \frac{1}{2} + \frac{1}{2}\sum_{i=1}^{Q} m_i \cos\left(\omega_i t + \phi_{i0} + (k-1)i\alpha\right) \tag{31}$$

where m_i, ω_i, and ϕ_{i0} are the modulation index, the angular frequency, and the initial phase angle of each component, respectively.

From (31) and according to (20), the reference voltage remains in the linear region of the modulation index if

$$0 \leq \frac{1}{2} + \frac{1}{2}\sum_{i=1}^{Q} m_i \cos\left(\phi_i + (k-1)i\alpha\right) \leq 1 \tag{32}$$

for all values of k and ϕ_i, where $\phi_i = \omega_i t + \phi_{i0}$. Therefore, the following constraint applies for the modulation indexes of the multifrequency reference voltage:

$$\sum_{i=1}^{Q} |m_i| \leq 1 \tag{33}$$

which is equivalent to (22). The expression in (21) corresponding to single output frequency is obtained from (33), making all the modulation indexes but one equal to zero.

If the correction of the dwell time is performed, then the overmodulation condition in (26) applies. In this case, the reference voltage remains in the linear region of the modulation index if

$$-1 \leq \frac{1}{2}\sum_{i=1}^{Q} m_i\{\cos\left(\phi_i + (p-1)i\alpha\right) - \cos\left(\phi_i + (q-1)i\alpha\right)\} \leq 1 \tag{34}$$

where $v_r^p = \max_k(v_r^k)$ and $v_r^q = \min_k(v_r^k)$. Taking into account the identity $\cos 2a - \cos 2b = 2\sin(a+b)\sin(b-a)$, this expression can be rewritten as

$$-1 \leq \sum_{i=1}^{Q} m_i \sin\left(\phi_i + \frac{p+q-2}{2}i\alpha\right)\sin\left(\frac{q-p}{2}i\alpha\right) \leq 1. \tag{35}$$

The aforementioned condition has to be satisfied for all values of ϕ_i; thus

$$\sum_{i=1}^{Q} \left| m_i \sin\left(\frac{q-p}{2} i\alpha\right)\right| \leq 1. \tag{36}$$

Since the higher and the lower values of the reference phase voltage are not known in advance, all the combinations of p and q must be tested. Due to the properties of the sinusoidal functions, there are several combinations of p and q that provide the same constraints. Only the following N equations are independent:

$$\sum_{i=1}^{Q} |m_i \sin(ni\alpha/2)| \leq 1, \qquad \text{for } n = 1, \ldots, N \tag{37}$$

where $N = (P-1)/2$ if P is an odd number and $N = P/2$ if P is an even number. The aforementioned expressions are equivalent to the expressions in (28). Equation (27) corresponding to single output frequency is obtained from (37) by making all the modulation indexes but m_1 equal to zero. Among the N conditions in (37), the most restrictive one is obtained for $n = N$. If P is an odd number, then $m_1 \leq 1/\sin(((P-1)/P)(\pi/2)) = 1/\cos(\pi/2P)$, and if P is an even number, then $m_1 \leq 1/\sin(\pi/2) = 1$.

REFERENCES

[1] E. Levi, R. Bojoi, F. Profumo, H. A. Toliyat, and S. Williamson, "Multiphase induction motor drives—A technology status review," *IET Elect. Power Appl.*, vol. 1, no. 4, pp. 489–516, Jul. 2007.

[2] E. Levi, "Multiphase electric machines for variable-speed applications," *IEEE Trans. Ind. Electron.*, vol. 55, no. 5, pp. 1893–1909, May 2008.

[3] F. Terrien, S. Siala, and P. Noy, "Multiphase induction motor sensorless control for electric ship propulsion," in *Proc. IEE PEMD*, Edinburgh, U.K., Mar. 31–Apr. 2, 2004, vol. 2, pp. 556–561.

[4] D. Gritter, S. Kalsi, and N. Henderson, "Variable speed electric drive options for electric ships," in *Proc. IEEE ESTS*, Philadelphia, PA, 2005, pp. 347–354.

[5] L. Parsa and H. A. Toliyat, "Five-phase permanent magnet motor drives for ship propulsion applications," in *Proc. IEEE ESTS*, Philadelphia, PA, Jul. 25–27, 2005, pp. 371–378.

[6] G. Atkinson, B. Mecrow, A. Jack, D. Atkinson, P. Sangha, and M. Benarous, "The design of fault tolerant machines for aerospace applications," in *Proc. IEEE IEMDC*, San Antonio, TX, May 15–18, 2005, pp. 1863–1869.

[7] J. Bennett, B. Mecrow, A. Jack, D. Atkinson, C. Sewell, G. Mason, S. Sheldon, and B. Cooper, "Choice of drive topologies for electrical actuation of aircraft flaps and slats," in *Proc. IEE PEMD*, Edinburgh, U.K., Mar. 31–Apr. 2, 2004, vol. 1, pp. 332–337.

[8] G. Atkinson, B. Mecrow, A. Jack, D. Atkinson, P. Sangha, and M. Benarous, "The analysis of losses in high-power fault-tolerant machines for aerospace applications," *IEEE Trans. Ind. Appl.*, vol. 42, no. 5, pp. 1162–1170, Sep./Oct. 2006.

[9] X. Huang, K. Bradley, A. Goodman, C. Gerada, P. Wheeler, J. Clare, and C. Whitley, "Fault-tolerant brushless dc motor drive for electro-hydrostatic actuation system in aerospace application," in *Conf. Rec. IEEE IAS Annu. Meeting*, Tampa, FL, Oct. 8–12, 2006, vol. 1, pp. 473–480.

[10] C. Gerada and K. J. Bradley, "Integrated PM machine design for an aircraft EMA," *IEEE Trans. Ind. Electron.*, vol. 55, no. 9, pp. 3300–3306, Sep. 2008.

[11] L. de Lillo, L. Empringham, P. W. Wheeler, S. Khwan-On, C. Gerada, M. N. Othman, and X. Huang, "Multiphase power converter drive for fault-tolerant machine development in aerospace applications," *IEEE Trans. Ind. Electron.*, vol. 57, no. 2, pp. 575–583, Feb. 2010.

[12] M. G. Simoes and P. Vieira, "A high-torque low-speed multiphase brushless machine—A perspective application for electric vehicles," *IEEE Trans. Ind. Electron.*, vol. 49, no. 5, pp. 1154–1164, Oct. 2002.

[13] S. Jiang, K. Chau, and C. Chan, "Spectral analysis of a new six-phase pole-changing induction motor drive for electric vehicles," *IEEE Trans. Ind. Electron.*, vol. 50, no. 1, pp. 123–131, Feb. 2003.

[14] R. Bojoi, A. Tenconi, F. Profumo, and F. Farina, "Dual-source fed multiphase induction motor drive for fuel cell vehicles: Topology and control," in *Proc. IEEE PESC*, Recife, Brazil, Jun. 11–16, 2005, pp. 2676–2683.

[15] S. Niu, K. Chau, D. Zhang, J. Jiang, and Z. Wang, "Design and control of a double-stator permanent-magnet motor drive for electric vehicles," in *Conf. Rec. IEEE IAS Annu. Meeting*, New Orleans, LA, Sep. 23–27, 2007, pp. 1293–1300.

[16] M. Steiner, R. Deplazes, and H. Stemmler, "New transformerless topology for ac-fed traction vehicles using multi-star induction motors," *EPE J. (Eur. Power Electron. Drives J.)*, vol. 10, no. 3/4, pp. 45–53, Sep. 2000.

[17] M. Abolhassani, "A novel multiphase fault tolerant high torque density permanent magnet motor drive for traction application," in *Proc. IEEE IEMDC*, San Antonio, TX, May 15–18, 2005, pp. 728–734.

[18] A. Iqbal, E. Levi, M. Jones, and S. N. Vukosavic, "Generalised sinusoidal PWM with harmonic injection for multi-phase VSIs," in *Proc. IEEE PESC*, Jeju, Korea, Jun. 18–22, 2006, pp. 2871–2877.

[19] O. Ojo and G. Dong, "Generalized discontinuous carrier-based PWM modulation scheme for multi-phase converter-machine systems," in *Conf. Rec. IEEE IAS Annu. Meeting*, Hong Kong, Oct. 2–6, 2005, vol. 2, pp. 1374–1381.

[20] D. Dujic, M. Jones, and E. Levi, "Continuous carrier-based vs. space vector PWM for five-phase VSI," in *Proc. Int. Conf. Comput. Tool EUROCON*, Warsaw, Poland, Sep. 9–12, 2007, pp. 1772–1779.

[21] D. Dujic, E. Levi, M. Jones, G. Grandi, G. Serra, and A. Tani, "Continuous PWM techniques for sinusoidal voltage generation with seven-phase voltage source inverters," in *Proc. IEEE PESC*, Orlando, FL, Jun. 17–21, 2007, pp. 47–52.

[22] P. de Silva, J. Fletcher, and B. Williams, "Development of space vector modulation strategies for five phase voltage source inverters," in *Proc. IEE PEMD*, Edinburgh, U.K., Mar. 31–Apr. 2, 2004, vol. 2, pp. 650–655.

[23] S. Xue and X. Wen, "Simulation analysis of two novel multiphase SVPWM strategies," in *Proc. IEEE ICIT*, Hong Kong, Dec. 14–17, 2005, pp. 1337–1342.

[24] H.-M. Ryu, J.-H. Kim, and S.-K. Sul, "Analysis of multiphase space vector pulse-width modulation based on multiple d-q spaces concept," *IEEE Trans. Power Electron.*, vol. 20, no. 6, pp. 1364–1371, Nov. 2005.

[25] S. Xue, X. Wen, and Z. Feng, "Multiphase permanent magnet motor drive system based on a novel multiphase SVPWM," in *Proc. CES/IEEE IPEMC*, Shanghai, China, Aug. 14–16, 2006, vol. 1, pp. 1–5.

[26] G. Grandi, G. Serra, and A. Tani, "Space vector modulation of a seven-phase voltage source inverter," in *Proc. SPEEDAM*, Taormina, Italy, May 23–26, 2006, pp. 1149–1156.

[27] G. Liliang and J. E. Fletcher, "A space vector switching strategy for 3-level 5-phase inverter drives," *IEEE Trans. Ind. Electron.*, vol. 57, no. 7, pp. 2332–2343, Jul. 2010.

[28] D. Dujic, G. Grandi, M. Jones, and E. Levi, "A space vector PWM scheme for multifrequency output voltage generation with multiphase voltage-source inverters," *IEEE Trans. Ind. Electron.*, vol. 55, no. 5, pp. 1943–1955, May 2008.

[29] M. J. Duran and E. Levi, "Multi-dimensional approach to multi-phase space vector pulse width modulation," in *Proc. IEEE IECON*, Paris, France, Nov. 7–10, 2006, pp. 2103–2108.

[30] M. Duran, S. Toral, F. Barrero, and E. Levi, "Real-time implementation of multi-dimensional five-phase space vector pulse-width modulation," *Electron. Lett.*, vol. 43, no. 17, pp. 949–950, Aug. 2007.

[31] A. Lega, M. Mengoni, G. Serra, A. Tani, and L. Zarri, "Space vector modulation for multiphase inverters based on a space partitioning algorithm," *IEEE Trans. Ind. Electron.*, vol. 56, no. 10, pp. 4119–4131, Oct. 2009.

[32] O. López, J. Alvarez, J. Doval-Gandoy, and F. D. Freijedo, "Multilevel multiphase space vector PWM algorithm," *IEEE Trans. Ind. Electron.*, vol. 55, no. 5, pp. 1933–1942, May 2008.

[33] O. López, J. Alvarez, J. Doval-Gandoy, and F. D. Freijedo, "Multilevel multiphase space vector PWM algorithm with switching state redundancy," *IEEE Trans. Ind. Electron.*, vol. 56, no. 3, pp. 792–804, Mar. 2009.

[34] J. I. León, O. López, L. G. Franquelo, J. Doval-Gandoy, S. Vázquez, J. Alvarez, and F. D. Freijedo, "Multilevel multiphase feedforward space-vector modulation technique," *IEEE Trans. Ind. Electron*, vol. 57, no. 6, pp. 2066–2075, Jun. 2010.

[35] E. Levi, D. Dujic, M. Jones, and G. Grandi, "Analytical determination of dc-bus utilization limits in multiphase VSI supplied ac drives," *IEEE Trans. Energy Convers.*, vol. 23, no. 2, pp. 433–443, Jun. 2008.

[36] Y. Zhao and T. Lipo, "Space vector PWM control of dual three-phase induction machine using vector space decomposition," *IEEE Trans. Ind. Appl.*, vol. 31, no. 5, pp. 1100–1109, Sep./Oct. 1995.

[37] G. Grandi, G. Serra, and A. Tani, "General analysis of multiphase systems based on space vector approach," in *Proc. EPE-PEMC*, Portoroz, Slovenia, Aug. 30–Sep. 1, 2006, pp. 834–840.
[38] E. Levi, M. Jones, S. N. Vukosavic, and H. A. Toliyat, "Operating principles of a novel multiphase multimotor vector-controlled drive," *IEEE Trans. Energy Convers.*, vol. 19, no. 3, pp. 508–517, Sep. 2004.
[39] A. Iqbal and E. Levi, "Space vector PWM for a five-phase VSI supplying two five-phase series-connected machines," in *Proc. IEEE PEMC*, Portoroz, Slovenia, Aug. 30–Sep. 1, 2006, pp. 222–227.
[40] E. Levi, M. Jones, S. N. Vukosavic, A. Iqbal, and H. A. Toliyat, "Modeling, control, and experimental investigation of a five-phase series-connected two-motor drive with single inverter supply," *IEEE Trans. Ind. Electron.*, vol. 54, no. 3, pp. 1504–1516, Jun. 2007.
[41] A. Iqbal, S. Vukosavic, E. Levi, M. Jones, and H. Toliyat, "Dynamics of a series-connected two-motor five-phase drive system with a single-inverter supply," in *Conf. Rec. IEEE IAS Annu. Meeting*, Hong Kong, Oct. 2–6, 2005, vol. 2, pp. 1081–1088.
[42] E. Levi, M. Jones, S. N. Vukosavic, and H. A. Toliyat, "Steady-state modeling of series-connected five-phase and six-phase two-motor drives," *IEEE Trans. Ind. Appl.*, vol. 44, no. 5, pp. 1559–1568, Sep./Oct. 2008.
[43] M. Jones, S. N. Vukosavic, D. Dujic, and E. Levi, "A synchronous current control scheme for multiphase induction motor drives," *IEEE Trans. Energy Convers.*, vol. 24, no. 4, pp. 860–868, Dec. 2009.
[44] M. Jones, D. Dujic, E. Levi, and S. N. Vukosavic, "Dead-time effects in voltage source inverter fed multi-phase ac motor drives and their compensation," in *Proc. Eur. Conf. Power Electron. Appl. EPE*, Barcelona, Spain, Sep. 8–10, 2009, pp. P.1–P.10, [CD-ROM].

Oscar López (M'05) received the M.Sc. and Ph.D. degrees from the University of Vigo, Vigo, Spain, in 2001 and 2009, respectively.

Since 2004, he has been an Assistant Professor with the Department of Electronics Technology, University of Vigo. His research interests are in the areas of ac power switching converters technology.

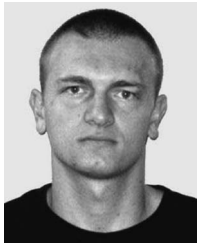

Drazen Dujic (S'03–M'09) received the Dipl.Ing. and M.Sc. degrees from the University of Novi Sad, Novi Sad, Serbia, in 2002 and 2005, respectively, and the Ph.D. degree from Liverpool John Moores University, Liverpool, U.K., in 2008.

From 2002 to 2006, he was a Research Assistant with the Department of Electrical Engineering, University of Novi Sad. From 2006 to 2009, he was a Research Associate with Liverpool John Moores University. He is currently with the ABB Corporate Research Center, Baden-Dättwil, Switzerland. His main research interests are in the areas of design and control of advanced power electronics systems and high-performance drives.

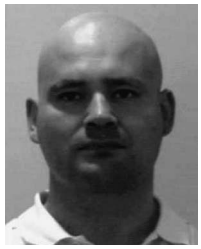

Martin Jones (M'07) received the B.Eng. degree (First Class Honors) and the Ph.D. degree from Liverpool John Moores University, Liverpool, U.K., in 2001 and 2005, respectively.

From September 2001 until Spring 2005, he was a research student at Liverpool John Moores University, where he is currently a Senior Lecturer.

Dr. Jones was a recipient of the IEE Robinson Research Scholarship for his Ph.D. studies.

Francisco D. Freijedo (M'07) received the M.Sc. degree in physics from the University of Santiago de Compostela, Santiago de Compostela, Spain, in 2002 and the Ph.D. degree from the University of Vigo, Vigo, Spain, in 2009.

Since 2005, he has been an Assistant Professor with the Department of Electronics Technology, University of Vigo. The areas of his research are quality problems, grid-connected switching converters, ac power conversion, and flexible ac transmission systems.

Jesús Doval-Gandoy (M'99) received the M.Sc. degree from the Polytechnic University of Madrid, Madrid, Spain, in 1991 and the Ph.D. degree from the University of Vigo, Vigo, Spain, in 1999.

From 1991 to 1994, he worked at industry. He is currently an Associate Professor with the University of Vigo. His research interests are in the areas of ac power conversion.

Emil Levi (S'89–M'92–SM'99–F'09) received the M.Sc. and Ph.D. degrees from the University of Belgrade, Belgrade, Yugoslavia, in 1986 and 1990, respectively.

From 1982 to 1992, he was with the Department of Electrical Engineering, University of Novi Sad, Novi Sad, Serbia. In May 1992, he joined Liverpool John Moores University, Liverpool, U.K., where he has been a Professor of electric machines and drives since September 2000.

Dr. Levi was the recipient of the IEEE Power and Energy Society's 2009 Cyril G. Veinott Award for contributions to electromechanical energy conversion. He serves as a Coeditor-in-Chief of the IEEE TRANSACTIONS ON INDUSTRIAL ELECTRONICS, as an Editor of the IEEE TRANSACTIONS ON ENERGY CONVERSION, and as a member of the Editorial Board of the *IET Electric Power Applications*.